JOURNAL OF CATALYSIS 133, 94–111 (1992)

Ni EXAFS Studies of the Ni–Mo–S Structure in Carbon-Supported and Alumina-Supported Ni–Mo Catalysts

S. P. A. LOUWERS AND R. PRINS

Technisch Chemisches Laboratorium, Eidgenössische Technische Hochschule, 8092 Zürich, Switzerland

Received August 20, 1990; revised March 25, 1991

Sulfided Ni–S/C, Ni–Mo–S/C, and Ni–Mo–S/Al_2O_3 catalysts were prepared by pore volume impregnation with a solution containing nitrilotriacetic acid, which gives almost exclusively the Ni–Mo–S structure. The catalysts were studied by means of *in situ* EXAFS measurements at the Ni K-edge. The Ni in the carbon-supported Ni catalysts was present in a Ni_3S_2-like phase. In the alumina-supported and carbon-supported Ni–Mo–S catalysts no bulk Ni sulfide was detected up to a Ni/Mo ratio of about 0.5, and all Ni was present at the Ni–Mo–S structure, which is the active phase in hydrodesulfurization. In this structure the Ni atoms are situated in a square pyramid of five S atoms at 2.22 Å, and have Mo neighbors at 2.85 Å. This indicates that the Ni atoms are situated on top of the S_4 squares at the MoS_2 edges in the Mo plane, in millerite-type Ni sites. A Ni–Ni coordination at 3.2 Å was observed at low Ni/Mo ratios, indicating that part of the Ni atoms are present at neighboring sites on the MoS_2 edge. In order to examine the influence of the H_2S partial pressure on the Ni structure, a Ni–Mo–S/Al_2O_3 catalyst was exposed to several flushing procedures after sulfidation. When the catalyst was flushed with a mixture of 2% H_2S or less in H_2, the Ni–S coordination number decreased, indicating that the Ni atoms become uncovered and are made available for catalysis.

INTRODUCTION

Although cobalt-promoted and nickel-promoted molybdenum sulfide catalysts have been used for many years in the hydrotreatment of petroleum feedstocks, the structure of these catalysts is at present not fully solved. It is known that the molybdenum in these catalysts is present in the form of MoS_2 crystallites, but consensus has not been reached yet over the cobalt or nickel structure, although much work has been done on this subject (*1–3*). While the exact position of the Ni or Co promoter remains unclear, it will not be possible to gain a complete understanding of their promotional effect.

In the past, several models have been proposed for the structural environment of the cobalt or nickel atoms. Lipsch and Schuit (*4*) and Schuit and Gates (*5*) suggested that in alumina-supported Co–Mo catalysts the MoO_3 monolayer, which is present after calcination, stays mainly intact and that during sulfidation some of the terminal oxygen ions are replaced by sulfur ions. The Co was thought to be located in the alumina, stabilizing the Mo oxo-sulfo-monolayer. Another model was presented by Voorhoeve and Stuiver (*6*). In this so-called intercalation model the molybdenum is present in MoS_2 crystallites, consisting of several MoS_2 slabs stacked on top of each other. The promoter atoms are situated in octahedral holes between the MoS_2 slabs. Later this model was modified by Farragher and Cossee (*7*), who proposed that the promoter atoms were only intercalated at the edges of the MoS_2 crystallite. Delmon and co-workers introduced a completely different model, the contact synergy model (*8, 9*). They observed that mixtures of bulk MoS_2 and Co_9S_8 exhibited a higher catalytic activity for hydrodesulfurization than the individual bulk sulfides, and therefore they concluded that in Co–Mo catalysts the Co and Mo are present as separate Co_9S_8 and MoS_2 phases. Promotion is thought to take place by spillover

0021-9517/92 $3.00

of hydrogen atoms created on Co_9S_8, to MoS_2, where the catalysis occurs.

At present the most widely accepted model is that of Topsøe and co-workers (*10–12*). In this model the catalytically active phase consists of a single-slab MoS_2 crystallite with cobalt or nickel atoms situated at the edges, decorating the Mo atoms. This structure is referred to as the "Co–Mo–S" or "Ni–Mo–S" structure. Many different Co and Ni positions are possible, however, along the MoS_2 edges. Mössbauer emission spectroscopy did not provide an answer as to where exactly the cobalt or nickel is located. Since no long-range order is present in these catalysts, techniques like XRD or electron diffraction cannot be used to answer this question. Since in extended X-ray absorption fine structure (EXAFS) spectroscopy only short range order is required (*13*), EXAFS is in principle a suitable technique for solving the local structure of the promoter atom. It has been found, however, that the Co–Mo–S or Ni–Mo–S structure is not the only structure in which the Co or Ni promoter may be found in the catalyst. The promoter has been found to form a bulk sulfide at the surface of the support, and in addition to this it has been shown that the promoter atoms may take up tetrahedrally coordinated sites in an Al_2O_3 support (*11*). The influence of these additional Ni or Co species on the EXAFS of the catalysts introduces difficulties into the evaluation of the structure of the catalytically active Co–Mo–S or Ni–Mo–S structure. The problem of Ni or Co dissolving into the Al_2O_3 can be overcome by using carbon instead of alumina as a support, since the promoter atoms do not dissolve into carbon. Furthermore, it is possible to prepare catalysts in which no bulk sulfides are present by using the method published by van Veen *et al.* (*14*). Recently we have presented preliminary EXAFS studies of catalysts prepared according to this method and have shown that Ni was present on the edge of MoS_2 particles in the Mo plane in a square pyramidal environment of sulfur atoms (*15, 16*). In this paper we give a full account of this work and extend it to several other Ni–Mo catalysts.

EXPERIMENTAL

Catalyst Preparation

A series of carbon-supported Ni–Mo catalysts with varying Ni/Mo ratios was prepared. The support used was a Lonza high-surface-area graphite (HSAG-300), which had a specific surface area of 300 m^2/g and a pore volume of 0.25 cm^3/g. Before use this carbon was treated with concentrated HNO_3 to remove Fe and Ca impurities. In addition two catalysts were prepared on Al_2O_3 (Condea Chemie, 0.53 cm^3/g, 233 m^2/g), which was used as received. All these carbon-supported and alumina-supported catalysts were prepared according to the method described by van Veen *et al.* (*14*), involving pore volume impregnation with a solution containing the appropriate amounts of NH_4OH (Fluka p.a.), MoO_3 (Fluka p.a.), $Ni(NO_3)_2 \cdot 6H_2O$ (Fluka p.a.), and nitrilotriacetic acid (NTA) (Merck p.a.). The molar ratio NTA/Mo was 1.1. After impregnation the catalysts were dried in air for 12 to 16 h at 120°C. The NTA-prepared catalysts will be denoted as Ni–Mo–S/C(x) and Ni–Mo–S/Al_2O_3(x), with x being the Ni/Mo atomic ratio. The Mo–S/C and Ni–S/C catalysts have been prepared according to the same preparation method, leaving out $Ni(NO_3)_2 \cdot 6H_2O$ or MoO_3, respectively.

Another series of Ni–Mo catalysts was prepared by pore volume impregnation of the Lonza HSAG-300 carbon support with a solution of $(NH_4)_6Mo_7O_{24} \cdot 4H_2O$, drying for 12–16 h at 120°C, subsequent pore volume impregnation with a solution of $Ni(NO_3)_2 \cdot 6H_2O$, and finally drying for 12–16 h at 120°C. These catalysts will be denoted as Ni–Mo/C(x). Compositions and notations of all catalysts are given in Table 1. It should be noted that none of the catalysts underwent calcination.

Catalytic Activity

The catalytic activities of the Ni–Mo/C catalysts for thiophene hydrodesulfuriza-

TABLE 1

Catalyst Composition and Notation

Catalyst	wt% Mo	wt% Ni	Ni/Mo atomic ratio	Notation
Ni–Mo/C	4.32	0.00	0.00	Mo–S/C
NTA	4.28	0.26	0.10	Ni–Mo–S/C(0.10)
prepared	4.37	0.80	0.30	Ni–Mo–S/C(0.30)
	4.11	1.21	0.48	Ni–Mo–S/C(0.48)
	4.38	2.07	0.77	Ni–Mo–S/C(0.77)
	4.40	3.39	1.25	Ni–Mo–S/C(1.25)
	0.00	1.48	∞	Ni–S/C
Ni–Mo/Al_2O_3	6.97	1.23	0.29	Ni–Mo–S/Al_2O_3(0.29)
NTA	7.01	2.43	0.56	Ni–Mo–S/Al_2O_3(0.56)
prepared				
Ni–Mo/C	4.41	0.26	0.10	Ni–Mo/C(0.10)
classically	4.41	0.80	0.30	Ni–Mo/C(0.30)
prepared	4.41	1.21	0.45	Ni–Mo/C(0.45)
	4.42	2.08	0.77	Ni–Mo/C(0.77)
	4.40	3.39	1.25	Ni–Mo/C(1.25)
	0.00	1.45	∞	Ni/C

tion were measured in a flow system incorporating a microreactor at atmospheric pressure. Catalyst samples of ca. 500 mg were sulfided in a flow of 60 cm^3/min of 10% H_2S in H_2 (Union Carbide, certified standard), which was led through a molecular sieve trap to remove any traces of water. During sulfidation the temperature was raised at a rate of 5°C/min to 400°C and then kept at this level for 2 h. Afterward a gas mixture consisting of 3% thiophene (Merck p.a.) in H_2 was introduced into the reactor at a flow of 60 cm^3/min. The hydrogen was led through a column filled with Pd/Al_2O_3 catalyst, which converted any traces of oxygen to water and subsequently through a molecular sieve column. Reaction products were analyzed by on-line gas chromatography. The thiophene conversion at steady state (typically after 2 h reaction time) was used to calculate a rate constant k_{HDS}, assuming first-order kinetics.

EXAFS

EXAFS spectra of all NTA-prepared catalysts were recorded at EXAFS station 9.2 at the Synchrotron Radiation Source (SRS) in Daresbury, United Kingdom. Catalyst samples were pressed into self-supporting wafers and mounted in an *in situ* EXAFS cell (*17*). The thickness of the samples was such that the absorption μx was 2.55, corresponding to an optimal signal to noise ratio. The samples were sulfided in a flow of 50 cm^3/min 10% H_2S in H_2. During this sulfidation the temperature was increased at a rate of 10°C/min to 400°C and then maintained at 400°C for 1 h. After this treatment, all catalysts but two were purged with He for 30 min at 400°C in order to remove all H_2S and subsequently cooled to room temperature under flowing He. In order to study the effect of the H_2S partial pressure two experiments with other pretreatments were carried out with the Ni–Mo–S/Al_2O_3(0.29) catalyst. Between the sulfidation with 10% H_2S and the He purging, a different gas was led over the catalyst for 30 min. In one case this gas consisted of 2% H_2S in H_2, in the other case of pure H_2. During all this time the temperature was kept at 400°C. After all pretreatments the EXAFS cell was cooled down and the X-ray absorption was measured at liquid nitrogen temperature.

In order to calculate phase shifts and backscattering amplitudes the EXAFS spectra of reference compounds were recorded. The reference compounds were pressed into self-supporting wafers with an absorbance μx of 2.55. If necessary BN was added as a binder. For the Ni–Mo contribution the NiMo coordination in $((C_6H_5)_4P)_2Ni(MoS_4)_2$ was used (*18*), and for the Ni–Ni contribution the Ni–Ni coordination in NiO was used (*19*). Finally, the Co–S coordination of CoS_2 was used for the Ni–S contribution (*20*). The use of a Co absorber instead of Ni is justified since Teo and Lee (*21*) showed that the phases of Co and Ni hardly differ. EXAFS spectra were recorded at liquid nitrogen temperature under a He atmosphere.

RESULTS

Catalytic Activity

The catalytic activities of all carbon-supported catalysts for thiophene HDS are presented in Table 2. In Fig. 1, k_{HDS} is plotted

TABLE 2

Catalytic Activity for Thiophene Hydrodesulfurization

Catalyst	k_{HDS} 10^{-3} m^3 s^{-1} kg^{-1}
Mo–S/C	1.00
Ni–Mo–S/C(0.10)	2.02
Ni–Mo–S/C(0.30)	3.44
Ni–Mo–S/C(0.48)	6.95
Ni–Mo–S/C(0.77)	5.27
Ni–Mo–S/C(1.25)	3.59
Ni–S/C	0.09
Ni–Mo/C(0.10)	1.60
Ni–Mo/C(0.30)	2.90
Ni–Mo/C(0.45)	3.25
Ni–Mo/C(0.77)	3.57
Ni–Mo/C(1.25)	3.00
Ni/C	0.20

as a function of the Ni/Mo atomic ratio. It is clear that Ni enhances the catalytic activity and that the activity reaches a maximum at a Ni/Mo ratio of 0.5 for the catalysts prepared with NTA, after which it gradually decreases. For the catalysts prepared without NTA the maximum in catalytic activity lies at a slightly higher Ni/Mo ratio. The activities of the NTA-prepared catalysts are higher than those of the classically prepared catalysts and the Ni/C and Ni–S/C catalysts have a very low activity.

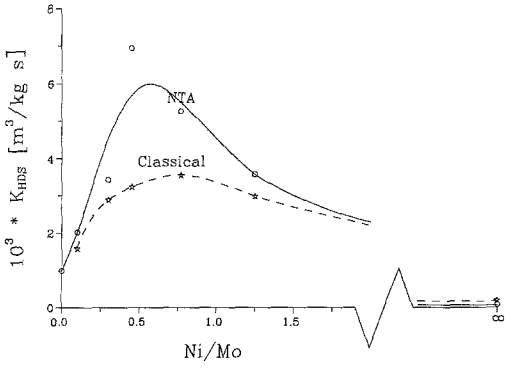

FIG. 1. First-order catalytic rate constants k_{HDS} of the Ni–Mo–S/C and Ni–Mo/C catalysts. (——) NTA-prepared catalysts. (– – –) Classically prepared catalysts.

TABLE 3

Ranges in k- and R-Space Used in the Analysis of the EXAFS Spectra

Catalyst	Range in k-space (Å^{-1})	Range in R-space (Å)
Ni–Mo–S/Al_2O_3(0.29)		
Ni–Mo–S/C(0.10)	3.75–11.03	0.70–3.30
Ni–Mo–S/C(0.30)	3.83–11.10	0.64–3.20
Ni–Mo–S/C(0.48)	3.68–11.00	0.62–3.20
Ni–Mo–S/C(0.77)	3.68–11.86	0.66–2.94
Ni–Mo–S/C(1.25)	3.64–12.00	0.52–3.04
Ni–S/C	3.20–11.50	0.55–3.58
Ni–Mo–S/Al_2O_3(0.29)	3.64–10.84	0.66–3.24
Ni–Mo–S/Al_2O_3(0.56)	3.64–10.84	0.74–3.16

EXAFS

The EXAFS functions of the NTA-prepared Ni–Mo and Ni catalysts were calculated by subtracting a quadratic expansion from the raw data, followed by a cubic spline background removal. Normalization was performed by division by the apparent edge height, which is obtained by back extrapolation of the EXAFS region. The EXAFS spectra were analyzed in the same way as in Refs. (*15*) and (*16*): High- and low-frequency noise, as well as higher shell contributions were removed by applying a Fourier transformation over as large a k-range as possible, while k_{min} and k_{max} were chosen in nodes of the experimental EXAFS functions, to minimize cut-off effects. The resulting radial distribution functions were backtransformed in the R-range of interest. The k- and R-ranges used in these procedure are given in Table 3. The thus obtained k^1- and k^3-weighted spectra were fitted in k- and R-space. The resulting structural parameters are presented in Table 4, while a comparison between the experimental data and the fit of the Ni–Mo–S/C(0.30) catalyst is given in Fig. 2 as an illustrative example.

In Table 5 and Fig. 3 the structural parameters resulting from the fit of the EXAFS data of the Ni–S/C catalyst are given. It is seen that the Ni–S/C catalyst has a Ni–S contribution with an atomic distance of

TABLE 4

Structural Parameters of the Ni–S, Ni–Ni, and Ni–Mo Coordinations for the Ni–Mo–S Catalysts

Catalyst	Ni–S coordination				Ni–Mo coordination			
	N^a	R^b Å	dw Å^2	E_0 eV	N^c	R^b Å	dw Å^2	E_0 eV
Ni–Mo–S/C(0.10)	5.3	2.22	0.0014	−3.0	1.5	2.86	0.0045	−12.8
Ni–Mo–S/C(0.30)	5.3	2.21	0.0024	−4.1	1.3	2.86	0.0061	−16.7
Ni–Mo–S/C(0.48)	5.4	2.22	0.0016	−0.8	0.8	2.84	0.0016	−13.7
Ni–Mo–S/C(0.77)	4.9	2.23	0.0028	−2.0	1.0	2.79	0.0071	−8.1
Ni–Mo–S/C(1.25)	4.9	2.23	0.0023	−0.9	0.5	2.77	0.0051	−4.0
Ni–Mo–S/Al_2O_3(0.29)	5.6	2.22	0.0023	−2.8	0.8	2.85	0.0027	−8.0
Ni–Mo–S/Al_2O_3(0.56)	5.2	2.24	0.0023	−2.1	1.0	2.82	0.0033	−10.8

Catalyst	Ni–Ni coordination				Ni–Ni coordination			
	N^c	R^b Å	dw Å^2	E_0 eV	N^c	R^d Å	dw Å^2	E_0 eV
Ni–Mo–S/C(0.10)	—	—	—	—	1.1	3.23	−0.0017	4.0
Ni–Mo–S/C(0.30)	—	—	—	—	0.6	3.15	−0.0018	12.9
Ni–Mo–S/C(0.48)	—	—	—	—	—	—	—	—
Ni–Mo–S/C(0.77)	0.4	2.58	0.0007	−9.4	Not analyzed			
Ni–Mo–S/C(1.25)	0.8	2.56	0.0024	−8.1	Not analyzed			
Ni–Mo–S/Al_2O_3(0.29)	—	—	—	—	1.0	3.21	0.0002	9.8
Ni–Mo–S/Al_2O_3(0.56)	—	—	—	—	—	—	—	—

Note. The coordination numbers have been corrected for the photoelectron mean free path dependence (λ = 5 Å).

[a] Inaccuracy, 20%.

[b] Inaccuracy, 2%.

[c] Inaccuracy, 50%.

[d] Inaccuracy, 5%.

2.25 Å, as well as a Ni–Ni contribution with an atomic distance of 2.56 Å. Two additional contributions are a Ni–S contribution at 3.56 Å and a Ni–Ni contribution at 3.72 Å. Concerning these last two contributions it should be noted that the inaccuracy in the structural parameters is rather large. This arises because, first, their EXAFS functions interfere with noise and, second, the atomic distances differ substantially from the atomic distances of the reference compounds. A third reason is that the R-range in the backtransformation of the radial distribution function could not be taken wider than 0.55–3.58 Å. Although the Ni–S contribution at 3.56 Å and the Ni–Ni contribution at 3.72 Å shift to lower R-values due to the phase shift, and the major part of these peaks is contained in this R-range, part of them exceed 3.58 Å and cut-off effects occur.

As can be seen from Table 4, the results show that there is no significant difference between the EXAFS structural parameters of the carbon-supported and alumina-supported Ni–Mo–S catalysts. All Ni–Mo catalysts contain a Ni–S contribution at about 2.22 Å and a Ni–Mo contribution around 2.8 Å. At low and high Ni/Mo ratios the spectra could not be fitted with only the Ni–S and Ni–Mo contribution. In both cases a Ni–Ni contribution had to be added

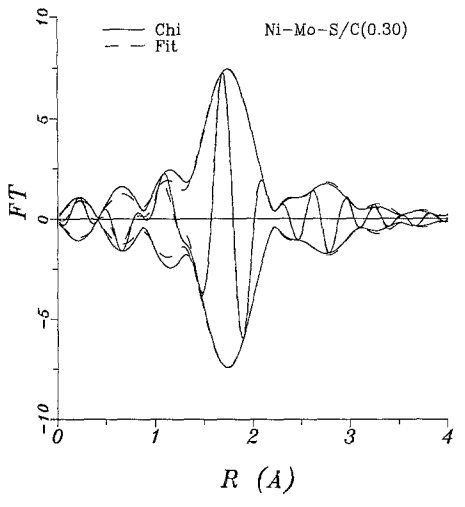

FIG. 2. Comparison between the k^3 Fourier-transformed (3.83–11.10 $Å^{-1}$) experimental Ni EXAFS data (solid line) and the corresponding calculated Fourier transform (dotted line) for the Ni–Mo–S/C(0.30) catalyst.

to obtain a good fit. This is illustrated in Fig. 4 for the Ni–Mo–S/C(0.10) catalyst and in Fig. 5 for the Ni–Mo–S/C(1.25) catalyst. As can be seen, fitting these catalysts with one Ni–S and one Ni–Mo contribution gave a poor result. Only after adding a Ni–Ni contribution with an atomic distance of 3.2 Å for the Ni/Mo = 0.1 catalyst and a distance of 2.58 Å for the Ni/Mo = 1.25 catalyst was the agreement between data and fit sufficient. Because of interference with higher shell contributions and high-frequency noise the inaccuracy in the structural parameters for this Ni–Ni contribution is relatively large. Since the data are not good enough to use more than three different contributions without violating the Brillouin theorem (*22*), and since there is a Ni–Ni coordination at 2.57 Å in the Ni–Mo–S/C(0.77) and Ni–Mo–S/C(1.25) catalysts, it was not possible to determine whether a Ni–Ni shell at 3.2 Å is present in these catalysts. It is worth mentioning that it has not been possible to fit the data beyond atomic distances of 3.2 Å, since the quality of the data is not good enough. First there is too much interference with high-frequency noise in that region, and second the number of contributions needed to obtain a reasonable fit is too high. For such a fit one needs more parameters than is allowed according to the Brillouin theorem.

The analysis showed that the Ni atoms were surrounded by five sulfur atoms. Since most fivefold coordinated complexes have a trigonal bipyramidal or square pyramidal structure, it seemed plausible that two separate Ni–S coordinations were present. Therefore the EXAFS of the Ni–Mo–S/C(0.48) catalyst was fitted with two Ni–S distances. The parameters resulting from this fit are given in Table 6. A comparison between experimental data and calculated spectra is given in Fig. 6. It can be seen that use of two Ni–S distances instead of one produces very little change in the quality of the fit. Furthermore the coordination numbers and atomic distances are not very different from the fit with one sulfur coordination. Therefore all catalysts have been analyzed with one Ni–S distance.

DISCUSSION

Ni–S/C and Ni/C

On the basis of the EXAFS results for Ni–S/C (Table 5), it is not absolutely clear what kind of nickel sulfide is present in this Ni–S/C catalyst. The inaccuracy associated with the coordination numbers predicted for

TABLE 5

Structural Parameters of the Ni–S and Ni–Ni Coordinations for the Ni–S/C Catalyst

Catalyst	Ni–S coordinations				Ni–Ni coordinations			
	N	*R* Å	*dw* Å²	E_0 eV	*N*	*R* Å	*dw* Å²	E_0 eV
Ni–S/C	3.5[a]	2.25[b]	0.0024	−0.1	1.8[a]	2.56[b]	0.0056	−2.6
	3.1[c]	3.56[d]	0.0099	12.0	1.4[c]	3.72[d]	0.0093	7.9

Note. The coordination numbers have been corrected for the photoelectron mean free path dependence (λ = 5 Å).

[a] Inaccuracy, 20%.

[b] Inaccuracy, 2%.

[c] Inaccuracy, 50%.

[d] Inaccuracy, 5%.

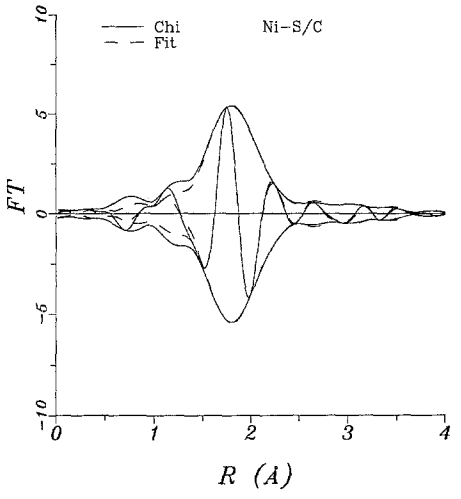

FIG. 3. Comparison between the k^3 Fourier-transformed (3.20–11.50 Å^{-1}) experimental Ni EXAFS data (solid line) and the corresponding calculated Fourier transform (dotted line) for the Ni–S/C catalyst.

the nickel sulfide is relatively large. This large inaccuracy coupled with the fact that the coordination numbers of small supported nickel sulfide particles can be very different from the coordination numbers in a similar bulk nickel sulfide means that it is safer to use the atomic distances for drawing conclusions about the kind of nickel sulfide present in the catalyst. The Ni–S atomic distance of 2.25 Å (Table 5) excludes the exclusive presence of NiS_2, $Ni_{17}S_{18}$, or NiS. These sulfides all have Ni–S distances larger than 2.3 Å, and also, the Ni–Ni atomic distance is much larger than 2.56 Å (*23–25*). For the latter reason one can also exclude Ni_3S_4, which has a minimum Ni–Ni atomic distance of 3.34 Å (*26*). Ni_7S_6 is not a very likely possibility either, since the second Ni–S distance encountered in our catalyst (3.56 Å) is definitely larger than the Ni–S distance of ca. 2.8 Å in Ni_7S_6 (*27*). The atomic distances agree well with the XRD data of Ni_3S_2 and Ni_9S_8 (*28, 29*). It is not possible to conclude whether the former or the latter phase dominates, but because Ni_3S_2 is the stable form under our preparation conditions, we assume that the nickel sulfide in our catalyst consists mainly of Ni_3S_2. The structural parameters of Ni_3S_2 are listed in Table 7.

The Ni–Ni coordination numbers found in the EXAFS analysis are much smaller

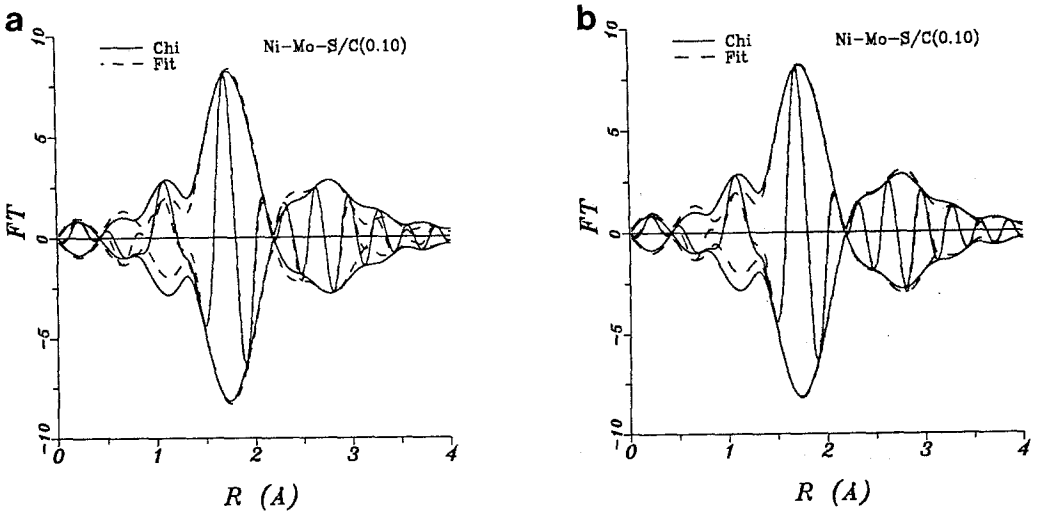

FIG. 4. Comparison of the k^3 Fourier-transformed (3.75–11.03 Å^{-1}) experimental Ni EXAFS data of the Ni–Mo–S/C(0.10) catalyst (solid line) and the corresponding calculated Fourier transform (dotted line). (a) Calculation with one Ni–S and one Ni–Mo contribution. (b) Calculation with one Ni–S, one Ni–Mo, and one Ni–Ni contribution.

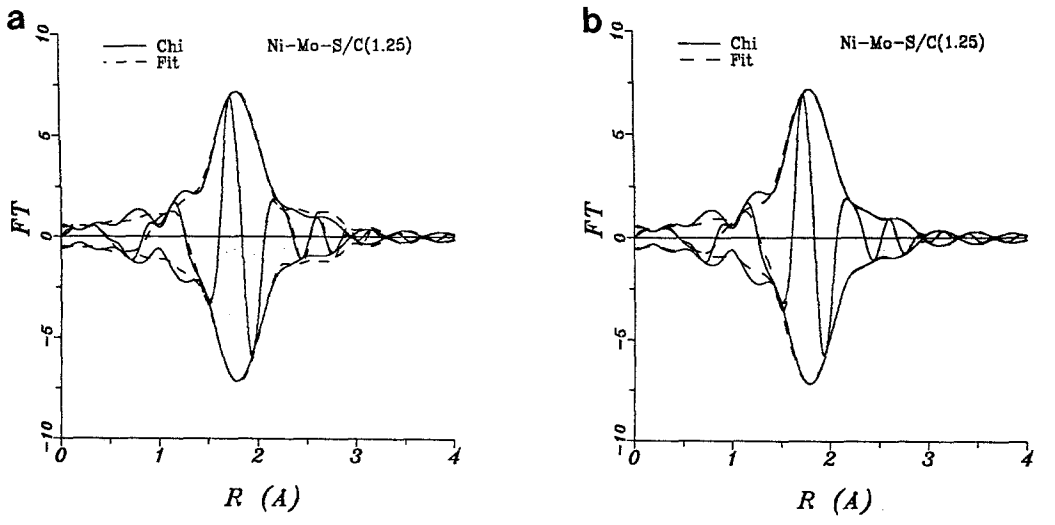

FIG. 5. Comparison of the k^3 Fourier-transformed (3.64–12.00 $Å^{-1}$) experimental Ni EXAFS data of the Ni–Mo–S/C(1.25) catalyst (solid line) and the corresponding calculated Fourier transform (dotted line). (a) Calculation with one Ni–S and one Ni–Mo contribution. (b) Calculation with one Ni–S, one Ni–Mo, and one Ni–Ni contribution.

than those for bulk Ni_3S_2. This means either that the Ni_3S_2 particles are very small or that they have a very limited ordering. Since one would expect high activities for catalysts with small Ni_3S_2 particles (as have been found on other carbon supports (*30*), with Ni also present in a Ni_3S_2-like phase) the fact that the catalytic activity is extremely low might suggest that the latter is the case. As far as the Ni–S/C and the Ni/C catalysts are concerned, the NTA recipe does not increase the activity of the catalysts. The rate constants k_{HDS} for both catalysts seem to be more or less the same within the limits of accuracy.

TABLE 6

Structural Parameters of the Ni–S and Ni–Mo Coordinations for the Ni–Mo–S/C(0.48) Catalyst Resulting from a Fit with Two Different Ni–S Contributions

Catalyst	Ni–S coordinations				Ni–Mo coordination			
	N^a	R^b Å	dw Å^2	E_0 eV	N^c	R^b Å	dw Å^2	E_0 eV
Ni–Mo–S/	3.8	2.22	0.0002	−1.1	0.8	2.84	0.0016	−12.9
C(0.48)	1.1	2.27	0.0024	−5.0				

Note. The coordination numbers have been corrected for the photoelectron mean free path dependence ($\lambda = 5$ Å).

[a] Inaccuracy, 20%.

[b] Inaccuracy, 2%.

[c] Inaccuracy, 50%.

Ni–Mo–S/C and Ni–Mo–S/Al_2O_3

At high Ni/Mo ratios a Ni–Ni coordination is seen with an atomic distance of 2.58 Å. As discussed in the previous paragraph this means that in these catalysts part of the Ni forms a Ni_3S_2-like phase. This is not observed at low Ni/Mo ratios. The fact that no Ni_3S_2 formation is seen up to a Ni/Mo ratio of 0.48 for the carbon-supported catalysts nor up to Ni–Mo = 0.56 for the alumina-supported ones, confirms that in these NTA-prepared catalysts only the Ni–Mo–S structure is formed. The catalysts prepared in the classical way (i.e., without NTA) have a lower activity, which might be due to the fact that NTA prevents the growth of MoS_2 particles. These MoS_2 crystallites could then be much smaller than in the classically prepared catalysts, thus giving rise to a higher activity. It might be argued that the mere fact that only Ni–Mo–S structure is formed could lead to a higher

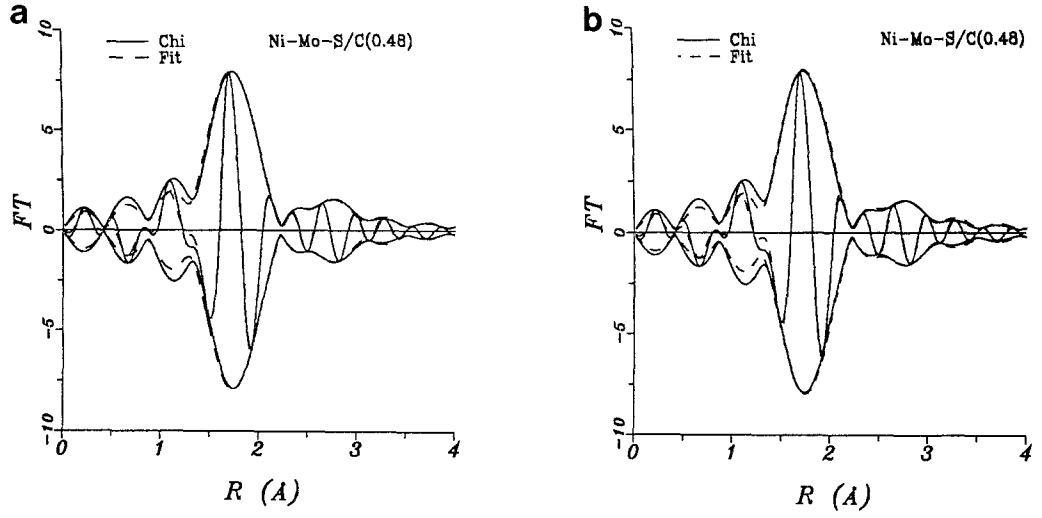

FIG. 6. Comparison of the k^3 Fourier-transformed (3.68–11.00 Å^{-1}) experimental Ni EXAFS data of the Ni–Mo–S/C(0.48) catalyst (solid line) and the corresponding calculated Fourier transform (dotted line). (a) Calculation with one Ni–S and one Ni–Mo contribution. (b) Calculation with two Ni–S and one Ni–Mo contributions.

activity, because no Ni would be present in catalytically inactive phases (Ni_3S_2 and Ni inside the Al_2O_3 support). However, since Topsøe *et al.* (*10*) did not find those phases in their classically prepared Co–Mo–S/Al_2O_3 catalysts up to a Co/Mo ratio of approximately 0.5, one can question this argument.

The formation of Ni sulfide at Ni/Mo ratios of 0.77 and higher in the NTA-prepared carbon-supported catalysts is not surprising, considering that at such high Ni loadings it is likely that not enough MoS_2 edge area is available for all Ni to form Ni–Mo–S. The surplus Ni will form a Ni sulfide. The formation of Ni_3S_2 or Ni_9S_8, as observed in the Ni–S/C catalyst, would account for the Ni–Ni contribution at 2.57 Å in the Ni–Mo–S/C(0.77) and Ni–Mo–S/C(1.25) catalysts. The formation of this separate nickel sulfide could also explain the apparent decrease in the Ni–S coordination number, since in both Ni_3S_2 and Ni_9S_8 every Ni has four sulfur neighbors at 2.25 Å. The peak at 2.22 Å might therefore represent a weighted average of 5.4 and four sulfur neighbors, resulting in a measured coordination number of 4.9.

TABLE 7

Crystallographic Data of Ni_3S_2

Coordination	Atomic distance Å	Coordination number
Ni–S	2.27	2
	2.29	2
Ni–Ni	2.48	2
	2.51	2
Ni–S	3.66	2
	3.69	2
Ni–Ni	3.79	4
	3.81	4

The observed Ni–S coordination distance of 2.22 Å and coordination number of 5.4 ± 1.0 for the Ni–Mo–S/C and Ni–Mo–S/Al_2O_3 catalysts agree very well with results obtained by other authors. Thus Niemann *et al.* (*31, 32*) observed that R = 2.22 Å and N = 4.7 ± 0.5 for the Ni–S coordination in a Ni–Mo/C catalyst and several groups reported a similar sulfur Co–S coordination in supported and unsupported sulfided Co–Mo catalysts (*33–37*). Deviat-

ing results have also been reported. Thus Bommannavar and Montano (*38*) did not find any evidence for a Ni–S coordination in a Ni–Mo/Al_2O_3 catalyst, probably because the sample was shortly exposed to the atmosphere between sulfidation and EXAFS measurements. Sankar *et al.* (*39*) observed a 10-fold coordination in their Co–Mo/Al_2O_3 catalyst, with N_{Co-S} = 6 at 2.33 Å and N_{Co-O} = 4 at 2.03 Å. This curious result must be due to the insufficient quality of their laboratory EXAFS data and limited analysis method. Chiu *et al.* (*40*) observed a Fourier transform peak at a distance shorter than the Co–S distance in Co_9S_8 as a consequence of incomplete sulfiding at 370°C of the Co–Mo/Al_2O_3 catalyst after a calcination at 550°C.

The observed Ni–Mo coordination proves that the Ni atoms are really linked to the MoS_2 structure, which is of importance because of some confusion in understanding the Mössbauer emission spectrum. Recently it was shown that pure cobalt sulfide supported on carbon exhibited the same MES signal as the Co–Mo–S structure (*41*), which implies that the occurrence of this MES signal cannot be taken as proof that the cobalt in sulfided Co–Mo/Al_2O_3 is connected to the MoS_2 crystallites (*42*). The present Ni–Mo results and also the recently observed Co–Mo coordination (*37*) in sulfided Ni–Mo and Co–Mo catalysts, however, constitute indisputable proof that the original suggestion of Ratnasamy and Sivasanker (*2*) and of Clausen *et al.* (*33*), that the Co and Ni are present at the edges of the MoS_2 crystallites, is valid. Nevertheless, even the rich information of three Ni–S, Ni–Mo, and Ni–Ni coordinations contained in the present EXAFS data is not sufficient to prove unequivocally, without further information or assumptions, in which sites these Ni atoms are located. The best one can do is to test existing and newly invented site models, discard the ones that are not in agreement with the EXAFS data, and retain the models that do not contradict the data. However, although such an agreement is necessary, it is not a sufficient proof for the correctness and uniqueness of the corresponding model.

Mo EXAFS measurements of sulfided Ni–Mo and Co–Mo HDS catalysts on different C and Al_2O_3 supports have shown that Mo in these catalysts is present as MoS_2, in which the Mo atoms are fully surrounded by sulfur (N_{Mo-S} = 6) (*16, 43*). Also on sulfided Ni–W catalysts, which have a structure similar to that of Ni–Mo catalysts, W–S coordination numbers of 6 have been found (*44*). It is therefore reasonable to assume that the same is true in our catalysts and that Mo forms hexagonal MoS_2 slabs and has a sulfur coordination number of 6. Farragher (*45*) showed that an electrically neutral MoS_2 edge cannot be fully saturated with S^{2-} sulfur ions. Because every Ni atom added to the MoS_2 edge only brings along one S atom, which is not enough to fully cover the MoS_2 edge, part of the sulfur ions is replaced by SH^- groups (two SH^- groups for one S^{2-} ion).

As discussed previously (*15, 16, 37, 46*), the observed structural parameters rule out the models suggested by Farragher and Cossee (*7*), Harris and Chianelli (*47*), and Ledoux *et al.* (*48*). The atomic distances, the coordination numbers, or both are not in agreement with these models. The Ni–S atomic distance of 2.22 Å agrees well with the literature value of 2.2 to 2.4 Å for cubane structures of Ni (or Fe or Co) with Mo and S (*49–52*). The Ni–Mo distance of 2.85 Å is a little long compared to the literature value of 2.7–2.8 Å, but not unreasonably so, and thus it might be argued that a type of cubane structure, as suggested by Chianelli *et al.* (*53*) and as shown in Fig. 7, could be formed on the MoS_2 edge. Examination of the Ni–Ni and Mo–Mo atomic distances shows, however, that a real cubane structure (i.e., a combination of a S_4 tetrahedron and a Ni_2Mo_2 tetrahedron) is not possible. The observed Ni–Ni atomic distance of 3.2 Å is larger than the value of about 2.8 Å that one would expect in a real cubane structure. The Mo–Mo atomic distance of 3.16 Å is also

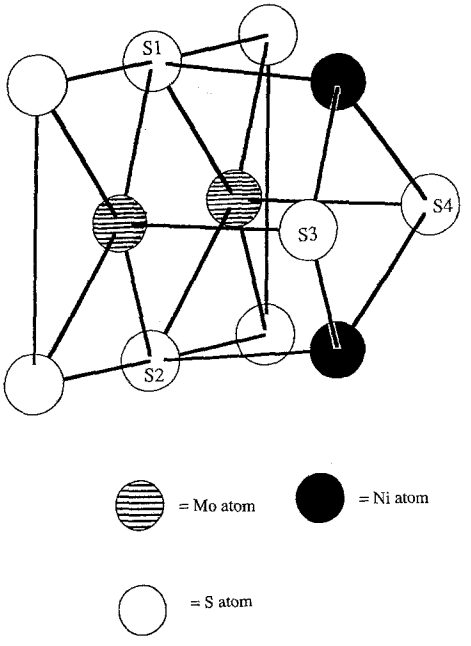

FIG. 7. Cubane-type structure on the MoS_2 edge.

too large to be present in a real cubane structure. It could be argued that a distorted cubane structure exhibiting larger Ni–Ni and Mo–Mo atomic distances than usual might be formed at the edge. However, in order for such a distorted structure to show agreement with the observed atomic distances, a large reconstruction of the MoS_2 crystallite would be required. This reconstruction would involve the Mo atoms at the edge of the crystallite moving 0.44 Å backward toward the crystallite. Such a large displacement of Mo atoms might be expected to have an influence on the Mo EXAFS of the catalysts, resulting in a variation in the observed Mo–Mo and Mo–S atomic distances. The fact that Mo EXAFS, performed by several authors (*16, 43, 46*) on catalysts similar to those employed in this study, have shown no such variations implies either that the cubane structure is very unlikely to occur or that the MoS_2 crystallites in these catalysts are so large that changes in the EXAFS due to reconstruction at the edge can be attenuated by the contribution of Mo atoms in the bulk of the crystallite. Finally, a further problem associated with the cubane structure is that in such a structure the S_3–S_4 atomic distance (Fig. 7) would have to be 2.94 Å. This is rather short compared to the more usual value of 3.5 Å. The above points taken together lead us to conclude that while we cannot totally exclude that a cubane site exists, we very much doubt its presence.

A model that is consistent with our EXAFS data is presented in Fig. 8. In this model the Ni atoms are located at substitutional sites on the MoS_2 edges. This idea was originally proposed by Ratnasamy and Sivasanker (*2*) and by Clausen *et al.* (*33*), and later worked out by the Topsøe group in a more detailed model (*32, 35*). The square pyramidal coordination of the Ni atoms resembles that of the millerite structure, which is given in Fig. 9 (*54*). They are connected to the MoS_2 crystallite by four sulfur atoms. An additional sulfur atom is attached in front of the Ni atom, as indicated in Fig. 8. This explains the Ni–S coordination number of 5.3. Mo EXAFS has shown that the Mo–S atomic distance is 2.41 Å, which is the same as that in bulk MoS_2. Only a small rearrangement of the MoS_2 edge is needed to obtain a structure in which the Ni–S, Ni–Mo, and Mo–S atomic distances can be met exactly. In this rearrangement the four edge-sulfur atoms must move 0.07 Å concertedly toward each other and 0.04 Å away from the MoS_2 edge. The Ni–Ni coordination at 3.2 Å can also be easily understood from this model; it represents a neighboring

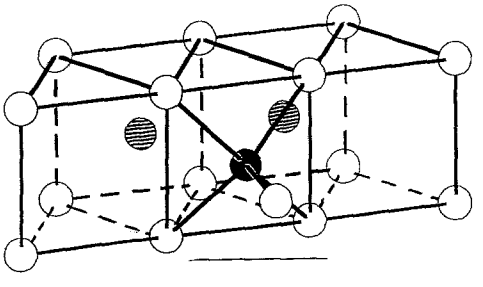

FIG. 8. Square pyramidal (millerite-type) site on an MoS_2 edge.

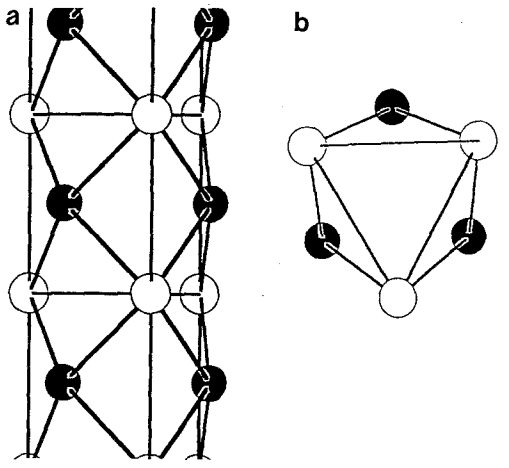

FIG. 9. Millerite structure. (a) Front view. (b) Top view.

Ni atom as indicated in Fig. 10. Sites of this kind are only possible on the $(10\bar{1}0)$ edge of an MoS_2 crystallite, and not on an unreconstructed $(\bar{1}010)$ edge. In view of the hexagonal shape of MoS_2 crystallites, it seems strange that all Ni can be accommodated at $(10\bar{1}0)$ planes, even up to Ni/Mo = 0.5. However, after a slight reconstruction the square pyramidal positions are also possible on the $(\bar{1}010)$ edge. This is illustrated in Figs. 11a and 11b, where the front view of an MoS_2 edge before and after reconstruction

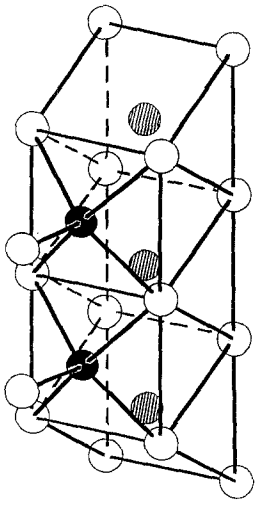

FIG. 10. Two neighboring square pyramidal coordinated Ni atoms, accounting for the Ni–Ni contribution at 3.2 Å.

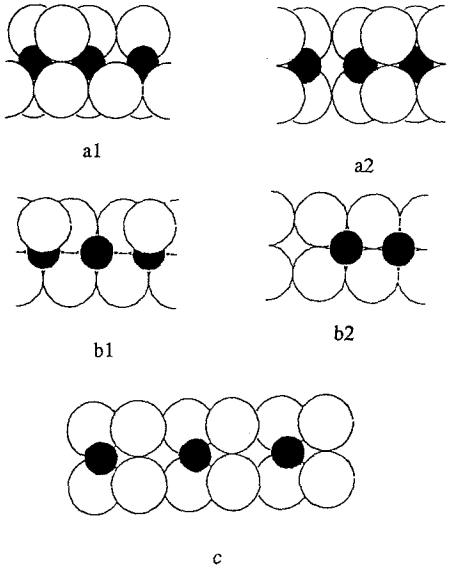

FIG. 11. Side view of the edges of a MoS_2 slab. (a1) Unreconstructed $(\bar{1}010)$ edge. (a2) Reconstructed $(\bar{1}010)$ edge. (b1) Unreconstructed $(10\bar{1}0)$ edge. (b2) $(10\bar{1}0)$ edge after removal of one MoS_2 unit. (c) Unreconstructed $(11\bar{2}0)$ edge.

is given. The $(10\bar{1}0)$ and $(\bar{1}010)$ edges are the most stable ones in bulk MoS_2. However, as Farragher (*45*) showed, the $(11\bar{2}0)$ edge (Fig. 11c) is only slightly less stable. Since it is not possible to put two Ni atoms on this edge at a distance of 3.2 Å, either this $(11\bar{2}0)$ edge is not present or it only takes up part of the Ni atoms.

According to this model one might expect to find a Ni–Mo contribution along the MoS_2 edge at 3.2 Å, as in Fig. 12. To check

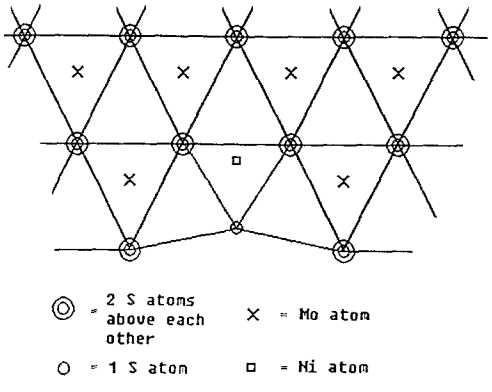

FIG. 12. Top view of the $(10\bar{1}0)$ edge of a MoS_2 slab.

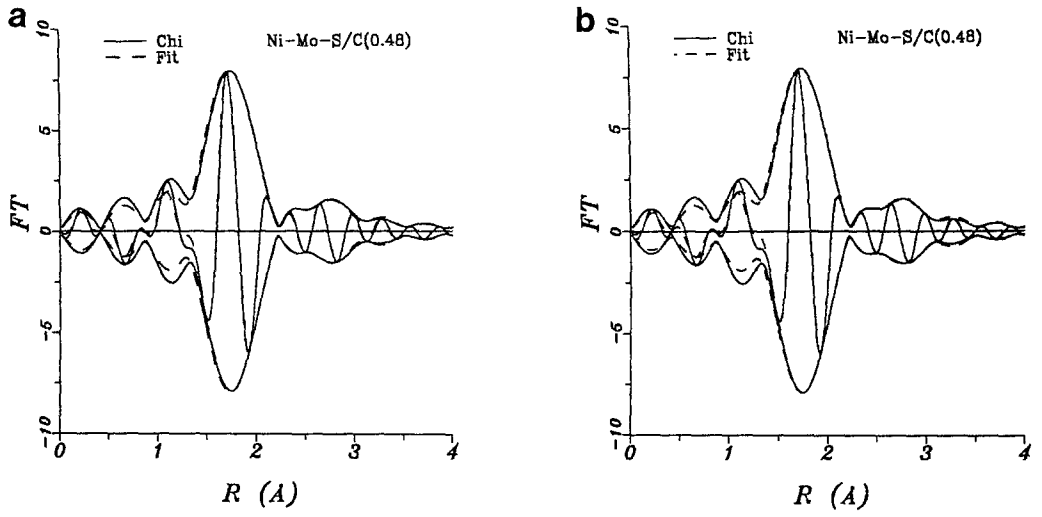

FIG. 13. Comparison of the k^3 Fourier-transformed (3.68–11.00 $Å^{-1}$) experimental Ni EXAFS data of the Ni–Mo–S/C(0.48) catalyst (solid line) and the corresponding calculated Fourier transform (dotted line). (a) Calculation with one Ni–S and one Ni–Mo contribution. (b) Calculation with one Ni–S and two Ni–Mo contributions, one of them at 3.2 Å.

whether this contribution is present the EXAFS data of catalyst Ni–Mo–S/C(0.48) were refitted, containing an additional Ni–Mo coordination at 3.2 Å. The results of the best fit are given in Fig. 13 and Table 8. As can be seen, adding this extra contribution does not lead to an increase in the quality of the fit. Also the corresponding Ni–Mo coordination number is rather low (N_{Ni-Mo} = 0.2). This, together with the fact that all catalysts can be fitted very well without this contribution, suggests that it is not present in large amounts. A reason for this might be the displacements of the edge sulfur atoms, necessary to accommodate the Ni promoter atoms. Because of this displacement a neighboring Mo atom cannot be positioned onto the MoS_2 edge with retention of the Mo–Mo and Mo–S atomic distances as in bulk MoS_2. Therefore this could give rise to a certain amount of strain, which makes a site neighboring the Ni atom energetically less favorable for Mo atoms. Thus it might be that the Ni atoms attach themselves onto a MoS_2 slab at sites with only few Mo neighbors.

TABLE 8

Structural Parameters of the Ni–S and Ni–Mo Coordinations for the Ni–Mo–S/C(0.48) Catalyst Resulting from a Fit with Two Different Ni–Mo Contributions

Catalyst	Ni–S coordination				Ni–Mo coordinations			
	N^a	R^b Å	dw Å^2	E_0 eV	N^c	R^b Å	dw Å^2	E_0 eV
Ni–Mo–S/C(0.48)	5.4	2.22	0.0016	−0.8	1.0	2.85	0.0039	−13.4
					0.2	3.16	0.0045	−15.3

Note. The coordination numbers have been corrected for the photoelectron mean free path dependence (λ = 5 Å).

[a] Inaccuracy, 20%.

[b] Inaccuracy, 2%.

[c] Inaccuracy, 50%.

One aspect of our data which is not in agreement with the square pyramidal model is the Ni–Mo coordination number. One would expect it to be 2, but we find N_{Ni-Mo} = 0.8–1.5. Why we find these small coordination numbers, while for Co–Mo catalysts Co–Mo coordination numbers of 2 have been found (*37*), is at present not clear. It might be that there is a substantial disorder in our catalysts, which together with an asymmetric distribution in the Ni–Mo atomic distance, might lead to an apparent loss in the coordination number (*55*).

As can be seen in Table 4 the Ni–Ni contribution at 3.2 Å decreases with increasing Ni content. A possible explanation for this is an increase in the structural disorder. If

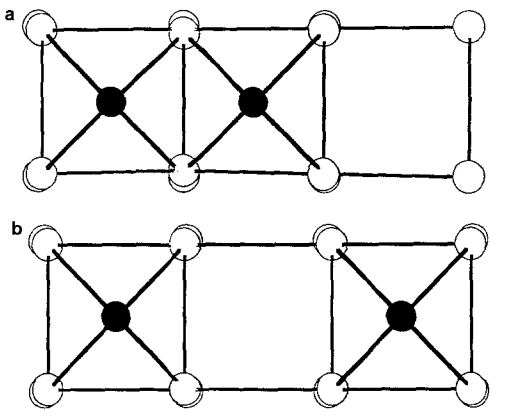

FIG. 14. Displacement of sulfur edge atoms. (a) Nickel atoms on neighboring sites. (b) Nickel atoms on separate sites.

more and more Ni atoms are added to the catalyst, it becomes increasingly difficult to disperse these atoms on the MoS_2 edge, since this involves a displacement of the sulfur edge atoms (*16*). If two Ni atoms are neighbors with an atomic distance of 3.2 Å, the displacement of the corresponding sulfur edge atoms is larger than in the case where these two Ni atoms are positioned further apart from each other. This is illustrated in Fig. 14 for the square pyramidal sites: the sulfur atoms in between the Ni atoms undergo a rearrangement considerably larger in Fig. 14a than in Fig. 14b. Therefore, the more Ni atoms are added, the larger the reconstruction that is needed, and the more likely it is that structural disorder occurs. If this disorder leads to an asymmetric distribution of atomic distances, this could, as mentioned above for the Ni–Mo contribution, lead to an apparent decrease in the Ni–Ni coordination number. In addition, the distribution of the Ni atoms over the $(10\bar{1}0)$ and $(\bar{1}010)$ edges may be dependent on the Ni/Mo ratio. As discussed before (*16*), the observed Ni–S and Ni–Mo distances lead to a position for the Ni atom that is 0.4 Å closer to the S_4 square than the position of a substitutional Mo atom would be. Therefore the distance between two neighboring Ni atoms on the $(\bar{1}010)$ edge (cf. Fig. 11 a2) should be 3.85 Å, rather than 3.16 Å as a bulk Mo–Mo distance and as a Ni–Ni distance along the $(10\bar{1}0)$ edge. The observation of a Ni–Ni distance at 3.2 Å at low Ni/Mo ratio therefore could mean that the Ni atoms prefer the $(10\bar{1}0)$ edge over the $(\bar{1}010)$ edge. The filling of sites on the $(\bar{1}010)$ edge at higher Ni/Mo ratios would then lower the average Ni–Ni coordination at 3.16 Å.

Another explanation could be a decrease in the MoS_2 particle size on increasing the amount of Ni, as other studies have suggested (*48, 56, 57*). The Ni atoms would then be distributed over a larger MoS_2 edge area, and the Ni–Ni coordination number would decrease. This seems to be contradictory to Mo EXAFS results of Bouwens *et al.* (*46*), who found a slight increase in the Mo–Mo coordination number on adding Ni or Co to Mo, indicating an increase in the MoS_2 particle size. Their results might, however, have been influenced by line dislocations in the MoS_2 structure (see Fig. 15). They would in that case not have measured the size of the MoS_2 particles, but the size of domains inside a MoS_2 particle.

Influence of the H_2S Partial Pressure

From the Ni–S coordination number found in this study and the Mo–S coordina-

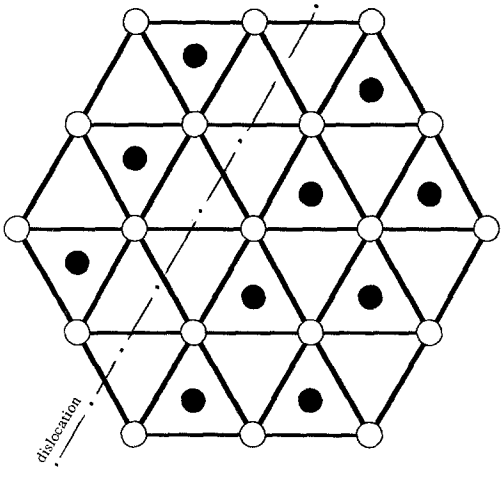

FIG. 15. MoS_2 slab with line dislocation.

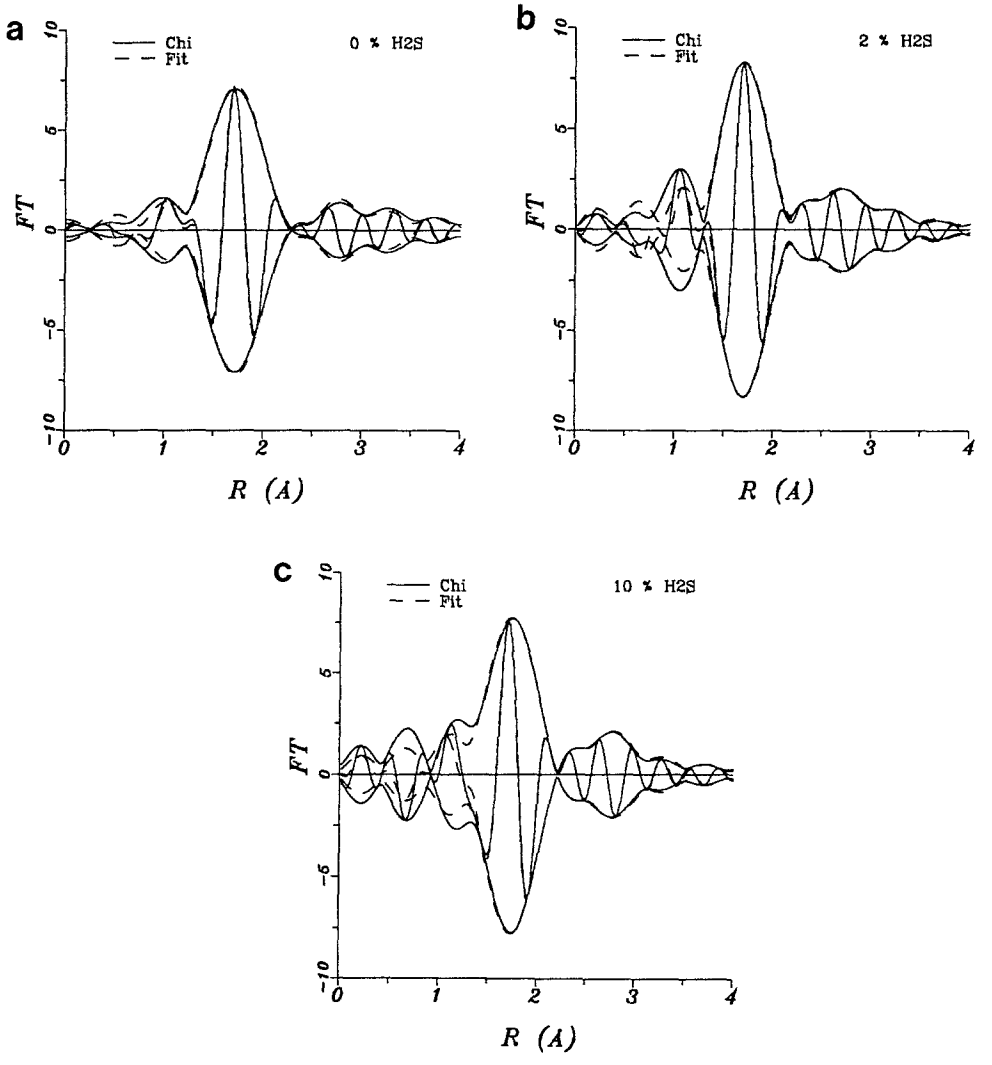

FIG. 16. Comparison between the experimental data (after Fourier transformation and backtransformation) and the calculated spectra for the catalyst Ni–Mo–S/Al_2O_3(0.29) after different pretreatments.

tion number of 6 obtained in Mo EXAFS studies (*16, 43, 44*) it appears as if all Mo and Ni atoms are fully coordinated with sulfur. If that is the case one wonders how these catalysts can be active in thiophene hydrodesulfurization. Indeed, if all sites were fully coordinated there would be no coordinatively unsaturated sites, which are generally accepted to be the sites where thiophene adsorbs (*6, 58–61*). On the other hand, it must be kept in mind that the catalysts have been sulfided in 10% H_2S in hydrogen and it might be that because of this high H_2S partial pressure the Ni and Mo atoms have high sulfur coordination numbers. The samples had undergone He flushing for a period of 30 min after sulfiding and before the EXAFS measurements, but this might only have removed gaseous or physisorbed H_2S, meaning that this flushing procedure has little influence on the sulfur coordination number. Under catalytic reaction conditions a gas mixture of 3% thiophene in hydrogen is led over the catalysts. Since only part of the

TABLE 9

Structural Parameters of the Ni–S, Ni–Mo, and Ni–Ni Coordinations for the Ni–Mo–S/Al(0.29) After Several Flushing Procedures

Flushing procedure	Ni–S coordination				Ni–Mo coordination			
	N^a	R^b Å	dw Å^2	E_0 eV	N^c	R^b Å	dw Å^2	E_0 eV
Only He flushing	5.6	2.22	0.0023	−2.8	0.8	2.85	0.0027	−8.0
2% H_2S/H_2	4.8	2.21	0.0003	1.7	1.4	2.81	0.0021	−9.4
H_2	4.8	2.22	0.0011	−0.8	1.1	2.80	0.0049	−3.7
	Ni–Ni coordination							
	N^c	R^d Å	dw Å^2	E_0 eV				
Only He flushing	1.0	3.21	0.0002	9.8				
2% H_2S/H_2	0.6	3.16	−0.0006	1.3				
H_2	0.6	3.23	−0.0009	7.1				

Note. The coordination numbers have been corrected for the photoelectron mean free path dependence (λ = 5 Å).

[a] Inaccuracy, 20%.

[b] Inaccuracy, 2%.

[c] Inaccuracy, 50%.

[d] Inaccuracy, 5%.

thiophene is converted into H_2S, the H_2S partial pressure during reaction is much smaller than during sulfidation. This could decrease the sulfur coordination number and thus create sites where thiophene can adsorb, explaining the catalytic activity.

In order to study this possibility the Ni–Mo–S/Al_2O_3(0.29) catalyst was investigated with EXAFS after three different flushing procedures. The first experiment was the standard experiment, in which the catalyst underwent only He flushing after sulfiding in 10% H_2S in H_2. These results have already been presented in Table 4. In a second experiment the He flushing was preceded by exposing the catalysts to a flow of 2% H_2S in H_2 for a period of 30 min, and in a third experiment the catalyst was exposed to a flow of pure hydrogen, again for a period of 30 min prior to He flushing. All gas velocities were 50 ml/min. The results are given in Fig. 16 and Table 9. Although it looks as if the Ni–S coordination numbers are the same within the absolute inaccuracy of 20%, the relative inaccuracy (one sample compared to another) is much better and is estimated to be 5%. Therefore it can be concluded that after flushing in 2% H_2S in H_2 the sulfur coordination number is indeed smaller. Flushing with H_2 instead of 2% H_2S in H_2 gives the same decrease in coordination number. At first sight it looks as if the new flushing methods also influence the Ni–Mo and Ni–Ni contributions. However, since these contributions are much smaller than the Ni–S contribution, N_{Ni-Mo} and N_{Ni-Ni} have inaccuracies much larger (absolute and relative) than that of N_{Ni-S}. It might be that within the limits of (absolute and relative) accuracy the N_{Ni-Ni} and N_{Ni-Mo} do not actually vary, and one cannot, therefore, draw any conclusions from the observed changes in these parameters.

CONCLUSIONS

By using EXAFS as a technique to characterize the local surrounding of Ni in a series of Ni-containing hydrodesulfurization

catalysts, it has been possible to obtain detailed structural information about the active phase in these catalysts. For the Ni–S/C catalyst it has been found that Ni is present in a Ni_3S_2-like phase. In the Ni–Mo–S/C and Ni–Mo–S/Al_2O_3 catalysts all Ni was present in a Ni–Mo–S structure up to a Ni/Mo ratio of 0.48 for the carbon-supported catalysts and up to a Ni/Mo ratio of 0.56 for the alumina-supported catalysts. The observation of a Ni–Mo coordination allowed us to prove that in this structure the Ni atoms are positioned at the outside of the MoS_2 crystallites in the Mo plane and that they are attached to a square of four sulfur atoms, which are part of the MoS_2 edge. A fifth sulfur atom is attached to the Ni atom, forming a square pyramidal coordination (Fig. 8). The Ni–S atomic distances are 2.22 Å. Also a Ni–Mo contribution is detected with an atomic distance of 2.85 Å, which represents the nearest Mo neighbors in the structure described above. Finally, a Ni–Ni coordination at 3.2 Å is observed at low Ni/Mo ratios, indicating that some Ni atoms are present at neighboring sites (Fig. 10). Our detailed results thus allow us to conclude that the suggestion made by Topsøe and co-workers for the location of the Co and Ni promoter atoms is indeed correct.

Flushing the Ni–Mo–S/Al_2O_3(0.10) catalyst with 2% H_2S in H_2 after sulfidation caused a decrease of the Ni–S coordination number, indicating that flushing uncovers the Ni atoms and makes them available for catalysis. Flushing with H_2 had the same effect.

ACKNOWLEDGMENT

We thank Prof. Dr. Ir. D. C. Koningsberger and co-workers from the Eindhoven University of Technology, The Netherlands, for the use of equipment and for their support with the EXAFS measurements and analyses.

REFERENCES

1. Prins, R., de Beer, V. H. J., and Somorjai, G. A., *Catal. Rev. Sci. Eng.* **31,** 1 (1989).
2. Ratnasamy, P., and Sivasanker, S., *Catal. Rev. Sci. Eng.* **22,** 401 (1980).
3. Grange, P., *Catal. Rev. Sci. Eng.* **21,** 135 (1980).
4. Lipsch, J. M. J. G., and Schuit, G. C. A., *J. Catal.* **15,** 179 (1969).
5. Schuit, G. C. A., and Gates, B. C., *AIChE J.* **19,** 417 (1973).
6. Voorhoeve, R. J. H., and Stuiver, J. C. M., *J. Catal.* **23,** 228, 236, 243 (1971).
7. Farragher, A. L., and Cossee, P., *in* "Proceedings, 5th International Congress on Catalysis, Palm Beach, 1972" (J. W. Hightower, Ed.), p. 1301. North-Holland, Amsterdam, 1973.
8. Hagenbach, G., Courty, Ph., and Delmon, B., *J. Catal.* **31,** 264 (1973).
9. Grange, P., and Delmon, B., *J. Less-Common Metals* **36,** 353 (1974).
10. Topsøe, H., Clausen, B. S., Candia, R., Wivel, C., and Mørup, S., *J. Catal.* **68,** 433 (1981).
11. Wivel, C., Candia, R., Clausen, B. S., Mørup, S., and Topsøe, H., *J. Catal.* **68,** 453 (1981).
12. Topsøe, N.-Y. and Topsøe, H., *J. Catal.* **84,** 386 (1983).
13. Stern, E. A., *in* "X-ray Absorption, Principles, Application, Techniques of EXAFS, SEXAFS, and XANES" (D. C. Koningsberger and R. Prins, Eds.), p. 4, Wiley, New York, 1988.
14. van Veen, J. A. R., Gerkema, E., van der Kraan, A. M., and Knoester, A., *J. Chem. Soc. Chem. Commun.*, 1684 (1987).
15. Louwers, S. P. A., and Prins, R., *Am. Chem. Soc. Div. Pet. Chem.* **35,** 211 (1990).
16. Bouwens, S. M. A. M., Koningsberger, D. C., de Beer, V. H. J., Louwers S. P. A., and Prins, R., *Catal. Lett.* **5,** 273 (1990).
17. Kampers, F. W. H., Maas, T. M. J., van Grondelle, J., Brinkgreve, P., and Koningsberger, D. C., *Rev. Sci. Instrum.* **60,** 2635 (1989).
18. Sotofte, I., *Acta Chem. Scand. A* **30,** 157 (1976).
19. Rooksby, H. P., *Acta Crystallogr.* **1,** 226 (1948).
20. Elliot, N., *J. Chem. Phys.* **33,** 903 (1960).
21. Teo, B. K., and Lee, P. A., *J. Am. Chem. Soc.* **101,** 2815 (1979).
22. Brillouin, L., "Science and Information Theory," 2nd ed. Academic Press, New York, 1962.
23. Bayliss, P., and Stephenson, N. C., *Mineral. Mag.* **36,** 940 (1968).
24. Collin, G., Chavant, C., and Comes, R., *Acta Crystallogr. B* **39,** 289 (1983).
25. Trahan, J., Goodrich, R. G., and Watkins, S. F., *Phys. Rev. B* **2,** 2859 (1970).
26. Lundqvist, P., *Ark. Kemi Mineral. Geol.* **24**(21), 1 (1947).
27. Fleet, M. E., *Acta Crystallogr. B* **28,** 1237 (1972).
28. Fleet, M. E., *Acta Crystallogr. C* **43,** 2255 (1987).
29. Westgren, A., *Z. Anorg. Chem.* **239,** 82 (1938).
30. de Beer, V. H. J., Duchet, J. C., and Prins, R., *J. Catal.* **72,** 369 (1981).
31. Niemann, W., Clausen, B. S., and Topsøe, H., *Catal. Lett.* **4,** 355 (1990).
32. Clausen, B. S., Niemann, W., Zeuthen, P., and

Topsøe, H., *Am. Chem. Soc. Div. Pet. Chem.* **35,** 208 (1990).
33. Clausen, B. S., Lengeler, B., Candia, R., Als-Nielsen, J., and Topsøe, H., *Bull. Soc. Chim. Belg.* **90,** 1249 (1981).
34. Clausen, B. S., Topsøe, H., Candia, R., and Lengeler, B., *Am. Chem. Soc., Symp. Ser.* **248,** 71 (1984).
35. Topsøe, H., Clausen, B. S., Topsøe, N.-Y., Pedersen, E., Niemann, W., Müller, A., Bögge, H., and Lengeler, B., *J. Chem. Soc. Faraday Trans. 1* **83,** 2157 (1987).
36. van Dijk, M. P., van Veen, J. A. R., Bouwens, S. M. A. M., van Zon, F. B. M., and Koningsberger, D. C., *in* "Proceedings, 2nd European Conference on Progress in X-ray Synchr. Rad. Research" (A. Balerna, E. Bernieri, and S. Mobilio, Eds.), Vol. 25, p. 139. SIF, Bologna, 1990.
37. Bouwens, S. M. A. M., van Veen, J. A. R., Koningsberger, D. C., de Beer, V. H. J., and Prins, R., *J. Phys. Chem.* **95,** 123 (1991).
38. Bommannavar, A. S., and Montano, P., *Appl. Surf. Sci.* **19,** 250 (1984).
39. Sankar, G., Vasudevan, S., and Rao, C. N. R., *J. Phys. Chem.* **91,** 2011 (1987).
40. Chiu, N.-S., Johnson, M. F. L., and Bauer, S. H., *J. Catal.* **113,** 281 (1988).
41. van der Kraan, A. M., Crajé, M. W. J., Gerkema, E., and Ramselaar, W. L. T. M., *Appl. Catal.* **39,** L7 (1988).
42. Karroua, M., Centeno, A., Matralis, H. K., Grange, P., and Delmon, B., *Appl. Catal.* **51,** L21 (1988).
43. Clausen, B. S., Topsøe, H., Candia, R., Villadsen, J., Lengeler, B., Als-Nielsen, J., and Christensen, F., *J. Phys. Chem.* **85,** 3868 (1981).
44. Kochubei, D. I., Kozlov, M. A., Zamaraev, K. I., Burmistrov, V. A., Strartsev, A. N., and Yermakov, Y. I., *Appl. Catal.* **14,** 1 (1985).
45. Farragher, A. L., *Adv. Colloid Interface Sci.* **11,** 3 (1979).
46. Bouwens, S. M. A. M., Prins, R., de Beer, V. H. J., and Koningsberger, D. C., *J. Phys. Chem.* **94,** 3711 (1990).
47. Harris, S., and Chianelli, R. R., *J. Catal.* **98,** 17 (1986).
48. Ledoux, M. J., Maire, G., Hantzer, S., and Michaux, O., *in* "Proceedings, 9th International Congress on Catalysis, Calgary, 1988" (M. J. Phillips and M. Ternan, Eds.), pp. 1–74. Chem. Institute of Canada, Ottawa, 1988.
49. Flank, A. M., Weininger, M., Mortenson, L. E., and Cramer, S. P., *J. Am. Chem. Soc.* **108,** 1049 (1986).
50. Carney, M. J., Papaefthymiou, G. C., Frankel, R. B., and Holm, R. H., *Inorg. Chem.* **28,** 1497 (1989).
51. Xinjian Lei, Zhiying Huang, Liu Qiutian, Maochung Hong, and Hanqin Liu, *Inorg. Chem.* **28,** 4302 (1989).
52. Zhang, Y., Bashkin, J. K., and Holm, R. H., *Inorg. Chem.* **26,** 694 (1987).
53. Chianelli, R. R., Daage, M., Halbert, T. R., Ho, T. C., and Stiefel, E. I., *Am. Chem. Soc. Div. Pet. Chem.* **35,** 227 (1990).
54. Alsen, N., *Geol. Foeren. Stockholm Foerh.* **47,** 19 (1925).
55. Eisenberger, P., and Brown, G. S., *Solid State Commun.* **29,** 481 (1979).
56. Pratt, K. C., and Saunders, J. V., *in* "Proceedings, 7th International Congress on Catalysis, Tokyo, 1980" (T. Seiyama and K. Tanabe, Eds.), p. 1420. Elsevier, Amsterdam, 1981.
57. Vrinat, M. L., and De Mourgues, L., *Appl. Catal.* **5,** 43 (1983).
58. Reddy, B. M., Chary, K. V. R., Rama Rao, B., Subrahmanyam, V. S., and Nag, N. K., *Polyhedron* **5,** 191 (1985).
59. Millman, W. S., Segawa, K., Smry, D., and Hall, K. W., *Polyhedron* **5,** 169 (1986).
60. Harris, S., and Chianelli, R. R., *J. Catal.* **86,** 400 (1984).
61. Konings, A. J. A., Valster, A., de Beer, V. H. J., and Prins, R., *J. Catal.* **76,** 466 (1982).